J. Iron Steel Res. Int. (2019) 26:1041–1051
https://doi.org/10.1007/s42243-018-0171-7

ORIGINAL PAPER

Kinetics of hot metal desulfurization using $CaO–SiO_2–Al_2O_3–Na_2O–TiO_2$ slag

Kang-hui Zhang[1] · Yan-ling Zhang[1] · Tuo Wu[1]

Received: 18 June 2018 / Revised: 30 September 2018 / Accepted: 2 October 2018 / Published online: 25 October 2018

Abstract
Kinetics of hot metal desulfurization were studied using $CaO–SiO_2–Al_2O_3–Na_2O–TiO_2$ slag in the range of 1400–1500 °C on a laboratory scale. The results of kinetic experiments indicate that the desulfurization rate increases as the temperature, Al_2O_3 content, Na_2O content, and TiO_2 content increase and basicity increases from 1.01 to 1.75, but decreases when basicity increases from 1.75 to 2.02. The melting effect of slag is promoted as the temperature, Na_2O content, and TiO_2 content increase and Al_2O_3 content increases from 12.13 to 17.17 mass%, but worsened as basicity increases and Al_2O_3 content increases from 17.17 to 22.27 mass%. A kinetic model of hot metal desulfurization has been developed to calculate the mass transfer coefficient and the mass transfer resistance of sulfur in slag. The mass transfer coefficient of sulfur increases as the temperature, Al_2O_3 content, Na_2O content, and TiO_2 content increase and basicity decreases. Total mass transfer coefficients of sulfur were in the range of (5.02–23.78) $\times$ 10^{-7} m s^{-1}. The activation energy was estimated to be 464.06 kJ mol^{-1} at the temperature from 1400 to 1450 °C and 176.35 kJ mol^{-1} at the temperature from 1450 to 1500 °C. The sulfur distribution at the slag–metal interface was observed using a mineral liberation analyzer. The result shows that the mass transfer of sulfur in slag is the controlling step at high temperature during the desulfurization process.

Keywords Hot metal desulfurization · Kinetics · Model · Liquid area · Kinetic parameter

1 Introduction

During the hot metal desulfurization process, the activity coefficient and the chemical potential of sulfur are larger in hot metal than in steel because of high carbon content. This is thermodynamically beneficial to desulfurization. However, the poor fluidity of desulfurizing slag typically limits the desulfurization efficiency in kinetics, particularly when using lime-based desulfurizer. This is caused by the lower temperature in the hot metal stage. Therefore, a desulfurizing slag with a much lower melting point, especially under the conditions of high basicity, is crucial for promoting the efficiency of hot metal desulfurization. Previous researches showed that Al_2O_3, Na_2O, and TiO_2 could lower the melting point and the viscosity of slag, and improve the kinetic conditions of desulfurization [1–9]. Pak and Fruehan [1] reported that the adding Na_2O lowered the melting point and improved the fluidity of lime-based slag. Zhang et al. [2] obtained good slag fluidity and a much better separation of metal from slag, attributed to the fact that Al_2O_3 and Na_2O could act as a flux and decrease the melting point of slag. Park et al. [3] and Xu et al. [4] reported that when Al_2O_3 content was greater than 10 mass%, the viscosity of molten slag decreased as Al_2O_3 content increased. Tang et al. [5] confirmed that when Al_2O_3 content was greater than 20 mass%, the viscosity of molten slag decreased with further increasing Al_2O_3 content. Yajima et al. [6] found that when Al_2O_3 was added to the $CaO–SiO_2–FeO_x$ slag system at an oxygen partial pressure of 1.8×10^{-3} Pa, the liquid areas became enlarged. Park et al. [7] measured the effect of TiO_2 content from 0 to 10 mass% on the viscosity of blast furnace slag. The viscosity of blast furnace slag decreased as TiO_2 content increased [7, 8]. Results of Fourier transform infrared (FTIR) and Raman spectroscopy confirmed that TiO_2 depolymerized the silicate network structure, which reduced the viscosity of blast furnace slag. Sohn et al. [9]

✉ Yan-ling Zhang
zhangyanling@metall.ustb.edu.cn

[1] State Key Laboratory of Advanced Metallurgy, University of Science and Technology Beijing, Beijing 100083, China

confirmed via X-ray photoelectron spectroscopy (XPS) analysis that TiO_2 decreased the slag viscosity by depolymerizing the silicate network structure. Therefore, Al_2O_3, Na_2O, and TiO_2 could lower the melting point and improve the desulfurization performance of slag. This is important for the hot metal desulfurization, particularly at the low temperature stage. Meanwhile, it could help users to avoid using CaF_2 [10] and realize fluoride-free steelmaking.

However, studies on the kinetics of hot metal desulfurization using slag that contains Al_2O_3, Na_2O, and TiO_2 are relatively limited [11, 12]. Choi et al. [11] studied the kinetics of hot metal desulfurization using CaO–SiO_2–Al_2O_3–Na_2O slag with basicity from 0.5 to 1.5 in the temperature range of 1270–1350 °C, and thought that the desulfurization is controlled either by the interfacial chemical reaction or slag phase mass transfer. Tong et al. [12] studied the kinetics of hot metal desulfurization using CaO–Al_2O_3–SiO_2–MgO–TiO_2–Na_2O slag with basicity from 2.46 to 3.46 in the temperature range of 1500–1560 °C, and thought that the desulfurization is controlled by the slag phase mass transfer. The present paper studies the kinetics of hot metal desulfurization using CaO–SiO_2–Al_2O_3–Na_2O–TiO_2 slag with basicity from 1.01 to 2.02 in the temperature range of 1400–1500 °C and adopts a different kinetic model of desulfurization.

In order to explore the feasibility of hot metal desulfurization using CaO–SiO_2–Al_2O_3–Na_2O–TiO_2-based flux, the liquid areas of CaO–SiO_2–Al_2O_3 slag system, along with the effects of Al_2O_3, Na_2O, and TiO_2, were initially investigated thermodynamically using FactSage7.0 software. Laboratory experiments were then performed to record the evolution of sulfur in hot metal with time, and the effects of various factors such as temperature and slag chemistry on the desulfurization rate were discussed. Finally, a kinetic model was developed to calculate the relevant kinetic parameters. The sulfur distribution at the slag–metal interface was observed by using a mineral liberation analyzer, and the controlling step during the desulfurization process was determined.

2 Liquid areas of CaO–SiO_2–Al_2O_3 (–Na_2O–TiO_2) slag system

As shown in Fig. 1, the FactSage7.0 software was used to simulate the liquid areas of CaO–SiO_2–Al_2O_3-based slag, and predict the effect of Al_2O_3, Na_2O, and TiO_2 on the melting properties of CaO–SiO_2–Al_2O_3 slag. In Fig. 1a, the liquid areas of CaO–SiO_2–Al_2O_3 slag at 1400 °C, 1500 °C, and 1600 °C account for about 1/11, 1/4, and 1/2 of the total diagram area, respectively. In Fig. 1a, there are three lines corresponding to the mass ratio of CaO to SiO_2 of 0.25, 1.00, and 4.00, respectively. When the mass ratio of CaO to SiO_2 is constant, the melting point of slag decreases at first and then increases with the addition of Al_2O_3, indicating that adding Al_2O_3 can promote the melting effect of slag at low concentrations and then deteriorate the melting effect after reaching a certain content. When the mass ratio of CaO to SiO_2 is 0.25, 1.00, and 4.00, the critical value of Al_2O_3 content is 13.7–19.3 mass%, 15.3–19.1 mass%, and 36.1–43.4 mass%, respectively. Figure 1b, c shows the effect of Na_2O and TiO_2 on the liquid areas of the CaO–SiO_2–Al_2O_3 slag at 1500 °C, respectively. Figure 1d shows the effect of the Na_2O and TiO_2 mixture (denoted as "NT") at a mass ratio of Na_2O to TiO_2 of 2 on the liquid areas of the CaO–SiO_2–Al_2O_3 slag at 1500 °C. The liquid areas enlarge with the increase in Na_2O, TiO_2, and NT contents, showing that they can all promote the melting of slag. However, Na_2O and NT can promote the melting of slag more effectively than TiO_2.

Therefore, when temperature is relatively low, the slag can also achieve good melting effect with adding Al_2O_3, Na_2O, and TiO_2, which is conducive to improving kinetics of desulfurization. In order to study the actual desulfurization rate of molten slag and obtain the related kinetic parameters, kinetic experiments of desulfurization were carried out.

3 Experimental

3.1 Experimental materials

The metal sample was prepared by melting iron from a blast furnace ironmaking works and high-purity FeS in an induction furnace. In order to obtain the obvious contrast effect, the sulfur content in hot metal for experiment was set as 0.36%, which is higher than that in normal hot metal, by referencing to previous research [12]. Its specific chemical compositions are shown in Table 1. In order to examine the effect of temperature (T), binary basicity [$R = w(CaO)/w(SiO_2)$], Al_2O_3, Na_2O, and TiO_2 on the desulfurization rate, some slags with various compositions were prepared by mixing the analytical grade reagents (CaO, SiO_2, Al_2O_3, Na_2SiO_3, and TiO_2). CaO, SiO_2, Al_2O_3, and TiO_2 were calcined at 1000 °C for 2 h, and Na_2SiO_3 was roasted at 300 °C for 2 h in a muffle furnace to remove carbonates and hydroxides prior to use. The slag was uniformly mixed in an agate mortar and then pre-melted in the molybdenum crucible in a resistance furnace at 1500 °C for 1 h. Compositions of the pre-melted slag are determined using an X-ray fluorescence spectrometer (XRF-1800) and shown in Table 2.

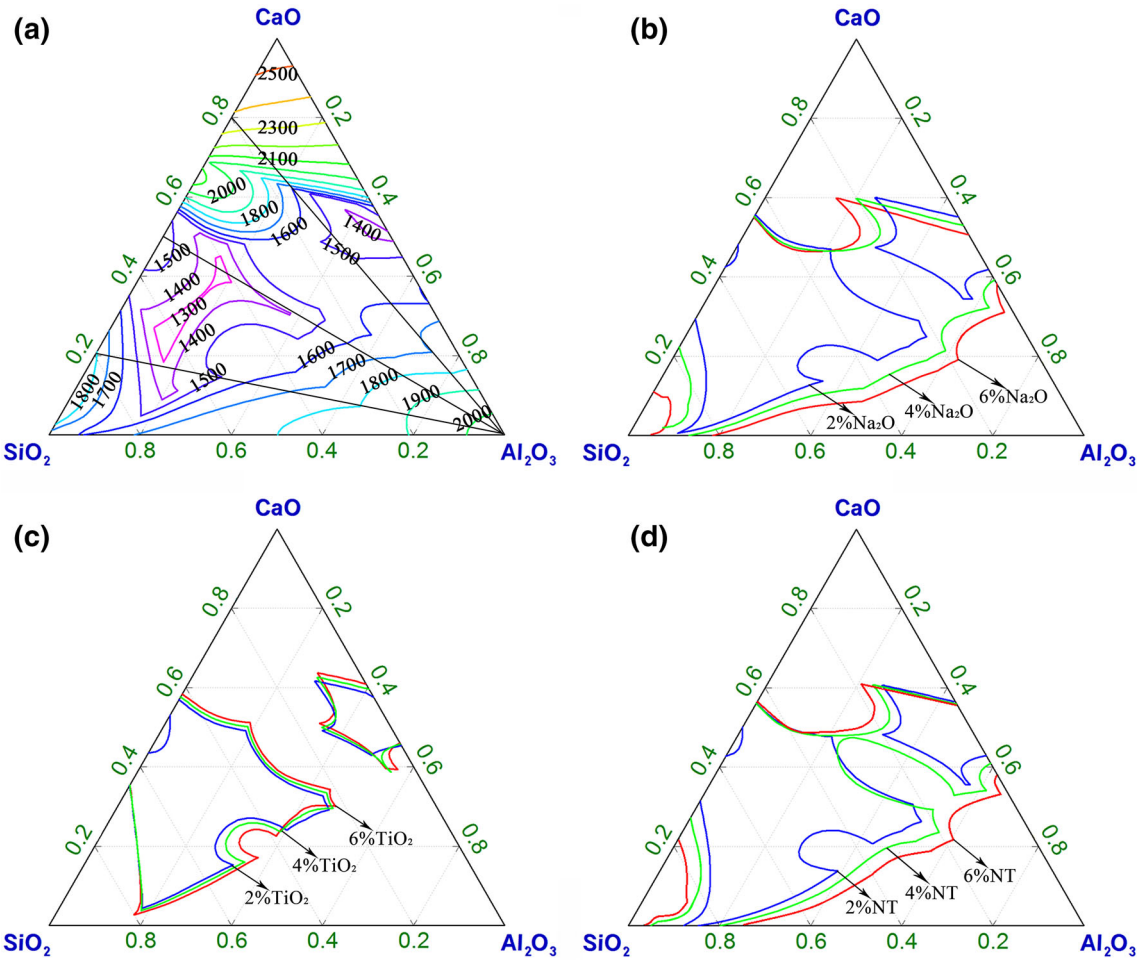

Fig. 1 Liquid areas of $CaO–SiO_2–Al_2O_3$ slag system between 1200 and 2600 °C (**a**) and effect of Na_2O (**b**), TiO_2 (**c**) and NT (**d**) on $CaO–SiO_2–Al_2O_3$ slag system at 1500 °C

Table 1 Chemical compositions of metal in the test (mass%)

Fe	C	Si	Mn	S	P
94.23	4.44	0.41	0.39	0.36	0.17

3.2 Experimental procedure

The laboratory experiments were performed in a vertical resistance furnace that was equipped with a gas-purification system and a water-cooling device. The schematic diagram of the experimental device is shown in Fig. 2. The furnace with $MoSi_2$ heating elements was controlled by a proportional–integral–derivative (PID) controller. Following calibration, a Pt-30%Rh/Pt-6%Rh thermocouple was used to measure temperature. The temperature control range of the furnace is 25–1700 °C, and the temperature accuracy of the heating zone is ± 2 °C. The water-cooling device was filled with circulating cooling water to control the temperature of the end of furnace tube. The gas-purification system consisted of allochroic silica gel, molecular sieve for dehydration, copper pieces, and magnesium pieces (heated to 500 °C) for deoxidation.

A graphite crucible (outer diameter of 60 mm, inner diameter of 50 mm, and height of 80 mm) with 200-g metal sample was positioned in the heating zone of the furnace. Ar gas was introduced into the furnace tube through the gas-purification system at the flow rate of 500 mL min^{-1}. The furnace was switched on and heated from room temperature to the target temperature at a heating rate of 5 °C min^{-1}. When the target temperature was reached, the initial metal sample was absorbed by a ϕ6-mm quartz suction tube, and the 60-g pre-melted slag was immediately added into the graphite crucible. After soaking for 5 min, it was taken as the starting time for kinetic study. Metal and slag samples were drawn at the predetermined time. The sulfur contents in slag and metal were detected using a carbon–sulfur analyzer (EMIA-920V2). The experimental results are shown in Table 3.

Table 2 Compositions of the pre-melted slag

Test No.	Temperature/°C	Basicity	CaO/mass%	SiO_2/mass%	Al_2O_3/mass%	Na_2O/mass%	TiO_2/mass%
T-1	1400	1.75	47.34	26.99	17.17	4.26	4.24
T-2	1430	1.75	47.34	26.99	17.17	4.26	4.24
T-3	1450	1.75	47.34	26.99	17.17	4.26	4.24
T-4	1470	1.75	47.34	26.99	17.17	4.26	4.24
T-5	1500	1.75	47.34	26.99	17.17	4.26	4.24
R-1	1450	1.01	37.41	37.11	17.20	4.13	4.15
R-2	1450	1.51	44.78	29.70	17.15	4.18	4.19
R-3	1450	1.75	47.34	26.99	17.17	4.26	4.24
R-4	1450	2.02	49.64	24.58	17.29	4.20	4.29
Al-1	1450	1.74	50.45	28.99	12.13	4.21	4.22
Al-2	1450	1.75	47.34	26.99	17.17	4.26	4.24
Al-3	1450	1.76	44.26	25.16	22.27	4.13	4.18
Na-1	1450	1.76	48.66	27.65	17.23	2.21	4.25
Na-2	1450	1.75	47.34	26.99	17.17	4.26	4.24
Na-3	1450	1.74	45.94	26.37	17.19	6.23	4.27
Ti-1	1450	1.76	48.69	27.70	17.26	4.18	2.17
Ti-2	1450	1.75	47.34	26.99	17.17	4.26	4.24
Ti-3	1450	1.76	46.15	26.21	17.13	4.31	6.20

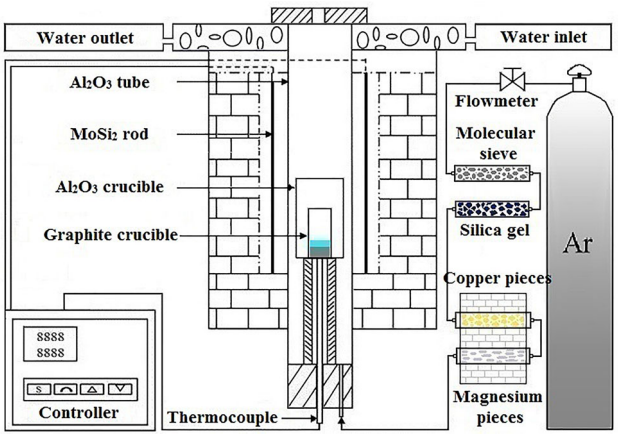

Fig. 2 Schematic diagram of experimental device

4 Results and discussion

4.1 Effect of different factors on desulfurization rate

Figure 3a shows the effect of temperature on the desulfurization rate. The sulfur content in hot metal decreases as temperature increases, suggesting that the desulfurization rate increases as temperature increases. The desulfurization reaction is endothermic. High temperature promotes the melting effect of slag and the migration of sulfur from metal into slag phase, which is beneficial for the desulfurization [13].

Figure 3b shows the effect of basicity on the desulfurization rate at 1450 °C. The desulfurization rate significantly increases when basicity increases from 1.01 to 1.75. The slag ion structure theory states that the concentration of the free O^{2-} in slag increases as basicity increases. The high concentration of the free O^{2-} promotes the desulfurization reaction and the depolymerization of the silicate structure; thus, the desulfurization rate increases [14]. However, the desulfurization rate decreases when basicity reaches 2.02. The reason is that the slag with higher basicity of 2.02 has a higher melting temperature, which results in a poor melting effect of slag, thus affecting the desulfurization rate.

Figure 3c shows the effect of Al_2O_3 content on the desulfurization rate at 1450 °C. The desulfurization rate obviously accelerates as Al_2O_3 content increases from 12.13 to 17.17%, and slightly increases when Al_2O_3 content increases from 17.17 to 22.27%. This result is contrary to the experimental results of Choi et al. [11] and Tong et al. [12]. Those studies state that the increasing Al_2O_3 was not conducive to the desulfurization rate. This opposite result can be explained by the amphoteric characteristics of Al_2O_3 in the aluminosilicate melts by using the FTIR spectra analysis. The infrared (IR) transmittance of slag as a function of the wavenumbers at various Al_2O_3 contents is shown in Fig. 4a. The Al_2O_3 addition results in the extension of the lower limit of IR bands for the $[AlO_4]$-tetrahedra from about 590 to 560 cm^{-1}, indicating that the polymerization degree of the aluminate decreases to some

Table 3 Experimental results of sulfur content in metal with time and in final slag (mass%)

Test No.	*w*([S]) at different time								*w*((S))
	0 min	5 min	10 min	20 min	30 min	40 min	50 min	3 h	
T-1	0.3706	0.3281	0.2898	0.2343	0.1897	0.1491	0.1295	0.0404	1.1647
T-2	0.3654	0.3073	0.2356	0.1614	0.0950	0.0686	0.0347	0.0346	1.1568
T-3	0.3516	0.2323	0.1719	0.0803	0.0534	0.0364	0.0328	0.0338	1.2586
T-4	0.3580	0.2277	0.1546	0.0561	0.0362	0.0319	0.0320	0.0324	1.2736
T-5	0.3777	0.2024	0.1266	0.0384	0.0333	0.0356	0.0316	0.0301	1.2483
R-1	0.3581	0.3016	0.2586	0.1903	0.1479	0.1302	0.1173	0.0984	0.9793
R-2	0.3618	0.2888	0.1982	0.1273	0.0881	0.0579	0.0500	0.0521	1.3440
R-3	0.3516	0.2323	0.1719	0.0803	0.0534	0.0364	0.0328	0.0338	1.2586
R-4	0.3613	0.2725	0.2394	0.1712	0.1282	0.1159	0.0985	0.0508	1.2600
Al-1	0.3687	0.3047	0.2667	0.2154	0.1844	0.1517	0.1322	0.0531	1.2005
Al-2	0.3516	0.2323	0.1719	0.0803	0.0534	0.0364	0.0328	0.0338	1.2586
Al-3	0.3800	0.2601	0.1710	0.0771	0.0521	0.0409	0.0357	0.0352	1.3037
Na-1	0.3707	0.3129	0.2505	0.1730	0.1087	0.0619	0.0316	0.0438	1.1281
Na-2	0.3516	0.2323	0.1719	0.0803	0.0534	0.0364	0.0328	0.0338	1.2586
Na-3	0.3655	0.1951	0.1035	0.0390	0.0287	0.0269	0.0269	0.0263	1.2105
Ti-1	0.3738	0.3046	0.2543	0.1981	0.1534	0.1278	0.0990	0.0396	1.1198
Ti-2	0.3516	0.2323	0.1719	0.0803	0.0534	0.0364	0.0328	0.0338	1.2586
Ti-3	0.3730	0.2664	0.1540	0.0443	0.0319	0.0309	0.0306	0.0303	1.2498

w([S]) and *w*((S)) are the concentration of sulfur in metal and in slag, respectively

extent. Therefore, the viscosity of slag and the mass transfer resistance of sulfur decrease, and the desulfurization rate accelerates. Park et al. [3] measured the viscosity of $CaO–SiO_2–Al_2O_3$ slag and analyzed the amphoteric behavior of Al_2O_3 on the structure of molten slag via infrared spectra. When Al_2O_3 was less than 10%, it primarily existed as $[AlO_4]$-tetrahedra, which could be incorporated into the silicate network, resulting in an increased viscosity. When Al_2O_3 was more than 10%, the relative fraction of $[AlO_6]$-octahedron increased, which could depolymerize the silicate network, resulting in a decreased viscosity.

Figure 3d shows the effect of Na_2O content on the desulfurization rate at 1450 °C. The desulfurization rate accelerates as Na_2O content increases, which is consistent with the effect that basicity has on the desulfurization rate. This is because Na_2O is a strong basic oxide, and Na^+ tends to have a strong affinity to S^{2-}. The free O^{2-} provided by Na_2O could depolymerize the silicate network and reduce the viscosity of molten slag. Meanwhile, Na_2O could lower the melting point of lime-based slag, reduce the consumption of acid oxides to CaO, and increase the activity of CaO [15]. Therefore, the desulfurization capacity of slag is enhanced, and the desulfurization rate increases.

Figure 3e shows the effect of TiO_2 content on the desulfurization rate at 1450 °C. The desulfurization rate increases as TiO_2 content increases. This is contrary to the experimental result of Tong et al. [12]. They considered that the increased TiO_2 was not beneficial for the desulfurization rate. Figure 4b shows the FTIR result of slag samples with varying TiO_2 content. The depth of the vibration bands for the $[SiO_4]$-tetrahedra at about 1070–750 cm^{-1} and for $[AlO_4]$-tetrahedra at about 750–580 cm^{-1} becomes shallower with the addition of TiO_2. The decrease in trough depth indicates that TiO_2 depolymerizes the slag by modifying the silicate and aluminate network, and finally reduces the slag viscosity. Therefore, the mass transfer resistance of sulfur decreases and the desulfurization rate increases. Additionally, Park et al. [7] directly measured the effect of TiO_2 on the viscosity of blast furnace slag. The viscosity of blast furnace slag decreased as TiO_2 content increased. Their results of the FTIR and Raman spectroscopy confirmed that TiO_2 depolymerized the silicate network, thereby reducing the viscosity of blast furnace slag. Sohn et al. [9] also verified via XPS analysis that TiO_2 decreased the slag viscosity by depolymerizing the silicate network.

Every experiment was carried out for 3 h. However, concentration curves of sulfur in hot metal as a function of time within 50 min were shown for the sake of comparison in the present study. For all reactions, there was a tendency that the desulfurization rate was rapid in early stage, and then became increasingly slow until the end of experiments.

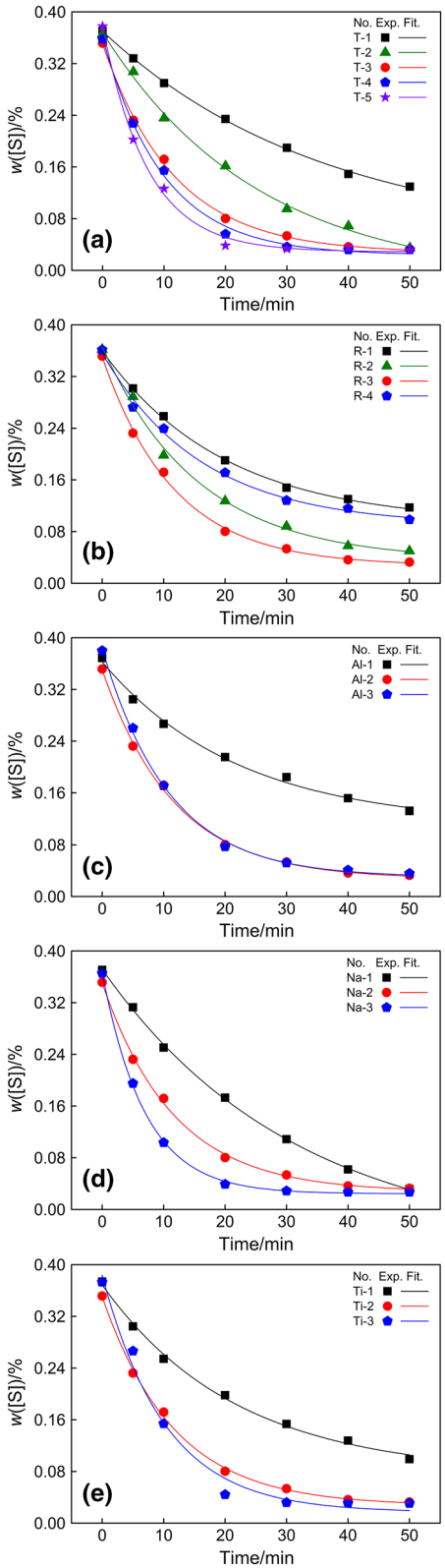

Fig. 3 Effect of different factors on desulfurization rate. **a** Temperature; **b** basicity; **c** Al_2O_3 content; **d** Na_2O content; **e** TiO_2 content

4.2 Kinetic model of desulfurization

According to the slag ion structure theory, the desulfurization reaction by slag can be expressed as:

$$[\mathrm{S}] + \left(\mathrm{O}^{2-}\right) = \left(\mathrm{S}^{2-}\right) + [\mathrm{O}] \tag{1}$$

The desulfurization reaction of hot metal is carried out at high temperature; thus, the chemical reaction is very quick and would not be a controlling step. The rate of change of sulfur in hot metal with time can be written as follows [16–18]:

$$-\frac{\mathrm{d}w([\mathrm{S}])}{\mathrm{d}t} = \frac{A}{W_\mathrm{m}} \frac{L_\mathrm{S} w([\mathrm{S}]) - w((\mathrm{S}))}{L_\mathrm{S}/(\rho_\mathrm{m} k_\mathrm{m}) + 1/(\rho_\mathrm{S} k_\mathrm{S})} \tag{2}$$

where L_S is the sulfur distribution ratio between the slag and hot metal; t is the reaction time, s; A is the reaction boundary area between the slag and hot metal, m^2; k_S and k_m are the mass transfer coefficients of sulfur in slag and hot metal, respectively, m s^{-1}; W_m is the mass of hot metal, kg; ρ_m and ρ_S are the density of hot metal and slag, respectively, kg m^{-3}; and $L_\mathrm{S}/(\rho_\mathrm{m} k_\mathrm{m})$ and $1/(\rho_\mathrm{S} k_\mathrm{S})$ can be considered as the mass transfer resistance of sulfur in hot metal and slag, respectively.

At the temperature of hot metal desulfurization, the viscosity of hot metal is about 1–2 orders of magnitude lower than that of molten slag; thus, the mass transfer in molten slag is often the controlling step [16]. In addition, the diffusion coefficient of oxygen is higher than that of sulfur in molten slag [12], meaning that the mass transfer rate of oxygen is quicker than that of sulfur in molten slag. Therefore, the mass transfer of sulfur in molten slag is generally considered to be the controlling step. Compared with the mass transfer resistance of sulfur in molten slag, the mass transfer resistance of sulfur in hot metal could be ignored.

Equation (2) can be simplified as Eq. (3):

$$-\frac{\mathrm{d}w([\mathrm{S}])}{\mathrm{d}t} = \frac{A}{W_\mathrm{m}} \frac{L_\mathrm{S} w([\mathrm{S}]) - w((\mathrm{S}))}{1/(\rho_\mathrm{S} k_\mathrm{S})} = \frac{A}{W_\mathrm{m}} \rho_\mathrm{S} k_\mathrm{S} \{L_\mathrm{S} w([\mathrm{S}]) - w((\mathrm{S}))\} \tag{3}$$

According to the principle of the conservation of mass, Eq. (4) could be derived for any given time t to be:

$$W_\mathrm{m}\{w([\mathrm{S}]_0) - w([\mathrm{S}])\} = W_\mathrm{S}\{w((\mathrm{S})) - w((\mathrm{S})_0)\} \tag{4}$$

That is,

$$w((\mathrm{S})) = \frac{W_\mathrm{m}}{W_\mathrm{S}}\{w([\mathrm{S}]_0) - w([\mathrm{S}])\} + w((\mathrm{S})_0) \tag{5}$$

where W_S is the mass of the slag, kg; and $w((\mathrm{S})_0)$ and $w([\mathrm{S}]_0)$ are the initial concentration of sulfur in slag and hot metal, respectively, mass%.

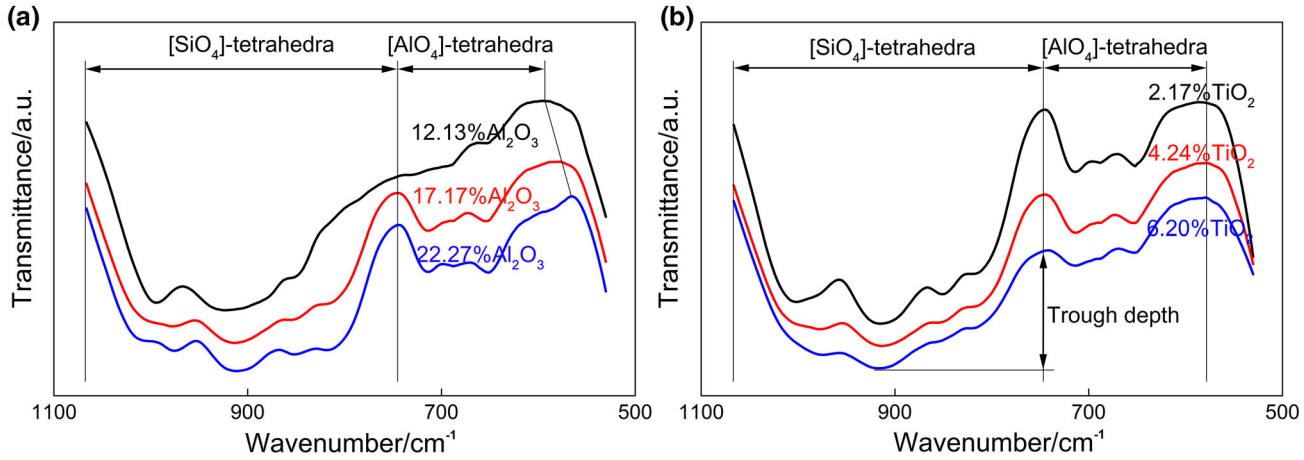

Fig. 4 FTIR result of slag samples with varying Al_2O_3 content (**a**) and TiO_2 content (**b**)

By substituting Eq. (5) into Eq. (3) and integrating from $w([S]_0)$ to $w([S])$, the kinetic equation for the change of sulfur content with time in hot metal can be obtained as follows:

$$w([S]) = \frac{\frac{W_m}{W_S} w([S]_0) + w((S)_0)}{L_S + \frac{W_m}{W_S}} + \frac{L_S w([S]_0) - w((S)_0)}{L_S + \frac{W_m}{W_S}} e^{-\frac{A}{W_m}\rho_S k_S \left(L_S + \frac{W_m}{W_S}\right) t} \quad (6)$$

Equation (6) can be rewritten as Eq. (7):

$$y = y_0 + a e^{bx} \quad (7)$$

where y represents $w([S])$; x represents time t; and the other three coefficients are expressed as follows:

$$y_0 = \frac{\frac{W_m}{W_S} w([S]_0) + w((S)_0)}{L_S + \frac{W_m}{W_S}} \quad (8)$$

$$a = \frac{L_S w([S]_0) - w((S)_0)}{L_S + \frac{W_m}{W_S}} \quad (9)$$

$$b = -\frac{A}{W_m} \rho_S k_S \left(L_S + \frac{W_m}{W_S}\right) \quad (10)$$

The experimental data are fitted by Origin8.0 software, and then, the mass transfer coefficient of sulfur in slag can be calculated. The fitting values are in good agreement with the experimental values, as shown in Fig. 3a–e, suggesting that the kinetic model is reasonable. After fitting and calculating, the relevant experimental parameters of kinetic model are shown in Table 4.

4.3 Effect of different factors on mass transfer coefficient and mass transfer resistance

The effects of temperature, basicity, Al_2O_3 content, Na_2O content, and TiO_2 content on the mass transfer coefficient and the mass transfer resistance of sulfur are shown in Fig. 5a–e, respectively.

As can be seen, the higher the temperature, the greater the mass transfer coefficient and the lower the mass transfer resistance, meaning that high temperature could lower the mass transfer resistance of sulfur. The mass transfer resistance decreases remarkably when temperature varies from 1400 to 1450 °C, but decreases slightly when temperature varies from 1450 to 1500 °C. This indicates that for the present slag system, 1450 °C is an ideal temperature, which can not only decrease the mass transfer resistance of sulfur and maintain a quicker desulfurization rate, but also avoid excessive temperature and save energy.

The mass transfer resistance increases as basicity increases. The reason is that the higher the basicity, the higher the melting temperature of slag, which leads to a worsening melting effect of slag and the greater mass transfer resistance of sulfur. The mass transfer resistance increases slowly as basicity increases from 1.01 to 1.75, but increases significantly when basicity increases from 1.75 to 2.02. This signifies that 1.75 is an ideal basicity for the present slag system, which could avoid the exorbitant mass transfer resistance of sulfur and maintain the strong desulfurization capacity.

The mass transfer resistance decreases as Al_2O_3 content increases. In experiment, it is found that the melting effect of slag is improved when Al_2O_3 increases from 12.13 to 17.17 mass% (Al-1, T-3), but worsened when Al_2O_3 increases from 17.17 to 22.27 mass% (T-3, Al-3). This demonstrates that 17.17 mass% is an ideal Al_2O_3 content for the present slag system, which maintains the low mass transfer resistance, while promoting the melting effect of slag.

The mass transfer resistance decreases as Na_2O content increases. In experiment, the higher Na_2O content improves the melting effect of slag (Na-1, T-3, Na-3).

Table 4 Experimental parameters used in the kinetic model

Test No.	L_S	ρ_S/(kg m^{-3})	A/mm^2	W_m/kg	W_S/kg	b	k_S/(m s^{-1})
T-1	28.83	2780	1963.5	0.2	0.06	2271.3	5.02×10^{-7}
T-2	33.43	2780	1963.5	0.2	0.06	1198.3	8.32×10^{-7}
T-3	37.24	2780	1963.5	0.2	0.06	683.78	1.321×10^{-6}
T-4	39.31	2780	1963.5	0.2	0.06	580.8	1.479×10^{-6}
T-5	41.47	2780	1963.5	0.2	0.06	437.6	1.869×10^{-6}
R-1	9.95	2780	1963.5	0.2	0.06	1160.2	2.378×10^{-6}
R-2	25.80	2780	1963.5	0.2	0.06	839.09	1.499×10^{-6}
R-3	37.24	2780	1963.5	0.2	0.06	683.78	1.321×10^{-6}
R-4	24.80	2780	1963.5	0.2	0.06	1275.6	1.021×10^{-6}
Al-1	22.61	2780	1963.5	0.2	0.06	2179.9	6.48×10^{-7}
Al-2	37.24	2780	1963.5	0.2	0.06	683.78	1.321×10^{-6}
Al-3	37.04	2780	1963.5	0.2	0.06	641.91	1.414×10^{-6}
Na-1	25.76	2780	1963.5	0.2	0.06	1234.3	1.020×10^{-6}
Na-2	37.24	2780	1963.5	0.2	0.06	683.78	1.321×10^{-6}
Na-3	46.03	2780	1963.5	0.2	0.06	415.61	1.786×10^{-6}
Ti-1	28.28	2780	1963.5	0.2	0.06	1662.4	6.97×10^{-7}
Ti-2	37.24	2780	1963.5	0.2	0.06	683.78	1.321×10^{-6}
Ti-3	41.25	2780	1963.5	0.2	0.06	598.17	1.374×10^{-6}

However, Na_2O easily corrodes the furnace lining, and vaporizes under high temperature and reduction conditions. Therefore, 4.26 mass% is an ideal Na_2O content for the present slag system.

The mass transfer resistance decreases as TiO_2 content increases. Additionally, the higher the TiO_2 content, the better the melting effect of slag (Ti-1, T-3, Ti-3) in the experiment. Therefore, 6.20 mass% is an ideal TiO_2 content for the present slag system.

Jung and Pak [19] studied the kinetics of hot metal desulfurization using CaO–CaF_2–Al_2O_3 slag, and the mass transfer coefficients of sulfur in slag were about (3.3–8.3) $\times$ 10^{-7} m s^{-1}. Choi et al. [11] studied the kinetics of hot metal desulfurization using CaO–SiO_2–Al_2O_3–Na_2O slag, and the mass transfer coefficients of sulfur in slag were about (15–30) $\times$ 10^{-7} m s^{-1}. The mass transfer coefficients of sulfur in the present study are (5.02–23.78) $\times$ 10^{-7} m s^{-1} and consistent with the results of previous studies [11, 19], suggesting that the present kinetic model is reasonable.

4.4 Activation energy

According to the Arrhenius equation [20],

$$k_S = k e^{-\frac{E_a}{R'T}} \tag{11}$$

where E_a is the activation energy, kJ mol^{-1}; R' is the universal gas constant, 8.314 J mol^{-1} K^{-1}; and k is pre-exponential constant, which is not related to the temperature.

Equation (12) can be derived from Eq. (11):

$$\ln k_S = -\frac{E_a}{R'T} + \ln k \tag{12}$$

The activation energy value can be calculated by the slope of the straight line, as shown in Fig. 6. The activation energy was 464.06 kJ mol^{-1} when temperature varied from 1400 to 1450 °C, and temperature has a great influence on the desulfurization rate. However, the activation energy was 176.35 kJ mol^{-1} when temperature varied from 1450 to 1500 °C, and temperature had little influence on the desulfurization rate. This result is related to the slag properties. Because of high viscosity of slag, the mass transfer resistance of sulfur is great at low temperature. The viscosity is lowered obviously when temperature increases. Therefore, temperature has a significant influence on the mass transfer resistance of sulfur, which is expressed as a relatively high activation energy value. However, the effect of temperature on the mass transfer resistance of sulfur weakens, because of low viscosity and good fluidity of slag at high temperature, which is expressed as a relatively low activation energy value.

According to Huang [16], the activation energy for the mass transfer in hot metal and slag is about 17–85 kJ mol^{-1} and 170–180 kJ mol^{-1}, respectively. Deo and Boom [21] reported that the activation energy ranged

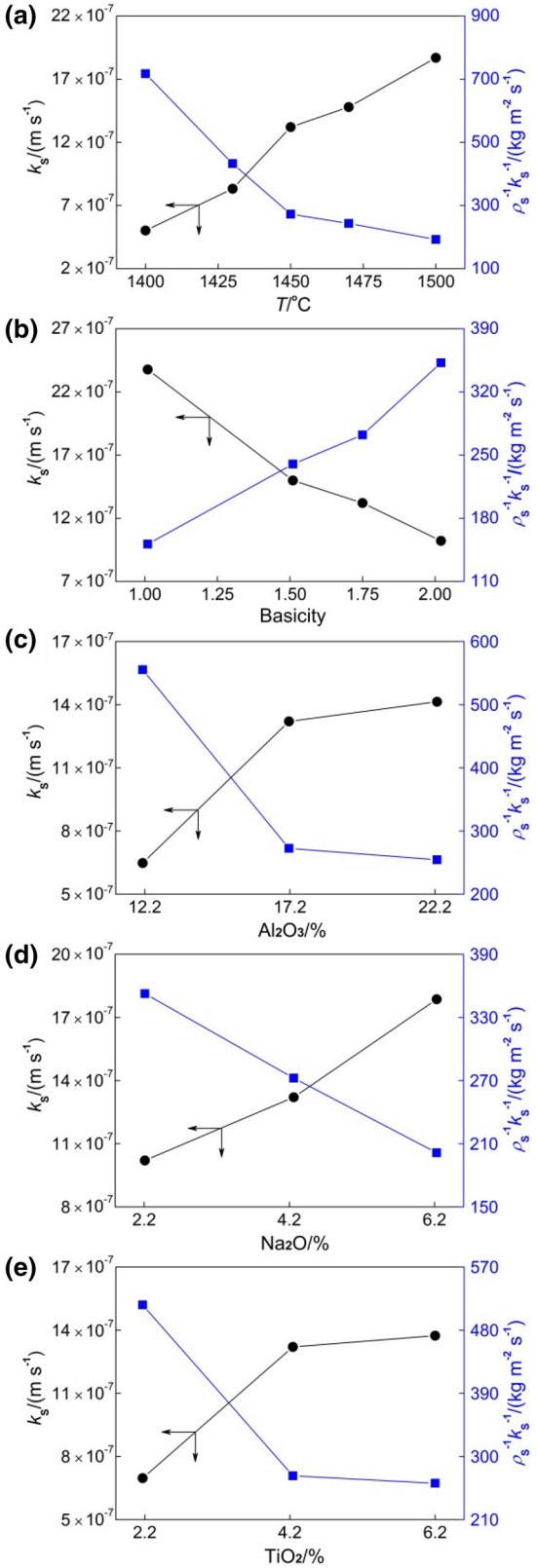

Fig. 5 Effect of different factors on mass transfer coefficient and mass transfer resistance. **a** Temperature; **b** basicity; **c** Al_2O_3 content; **d** Na_2O content; **e** TiO_2 content

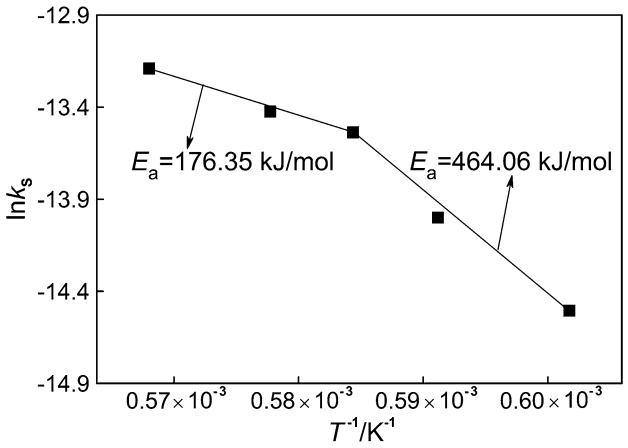

Fig. 6 Relationship between $\ln k_S$ and $1/T$

about 2400–3600 kJ mol^{-1} when the chemical reaction was the controlling step. The present study shows that the activation energy is 464.06 kJ mol^{-1} when temperature ranges from 1400 to 1450 °C, which is beyond the activation energy range of mass transfer restriction. The reason is that there are some solid particles in slag at the temperature from 1400 to 1450 °C, which leads to the controlling step of desulfurization between the mass transfer of slag phase and the interface chemical reaction. Tong et al. [12] have studied the kinetics of hot metal desulfurization in the range of 1500–1560 °C using $CaO–Al_2O_3–SiO_2–MgO–TiO_2–Na_2O$ slag. The activation energy was 172.58 kJ mol^{-1}, and the slag phase mass transfer was the controlling step, which is consistent with the current result at the high temperature stage.

4.5 Sulfur distribution at slag–metal interface

The sulfur distribution at the slag–metal interface observed using a mineral liberation analyzer (MLA250) is shown in Fig. 7. Figure 7a, b shows the scanning images of the micro-zone at the slag–metal interface with reaction time of 2 min and 40 min at 1450 °C, respectively. The left side with gray is the metal, the right side with black is the slag, and the middle thin line is the scanning line of sulfur content. The sulfur content on the slag side at the slag–metal interface has a sudden increase, and then gradually decreases from the left to the right in these two images. This suggests that there is a diffusion layer of sulfur on the slag side at the slag–metal interface, where sulfur is hindered and accumulated in this diffusion layer, which becomes a controlling step during the desulfurization process.

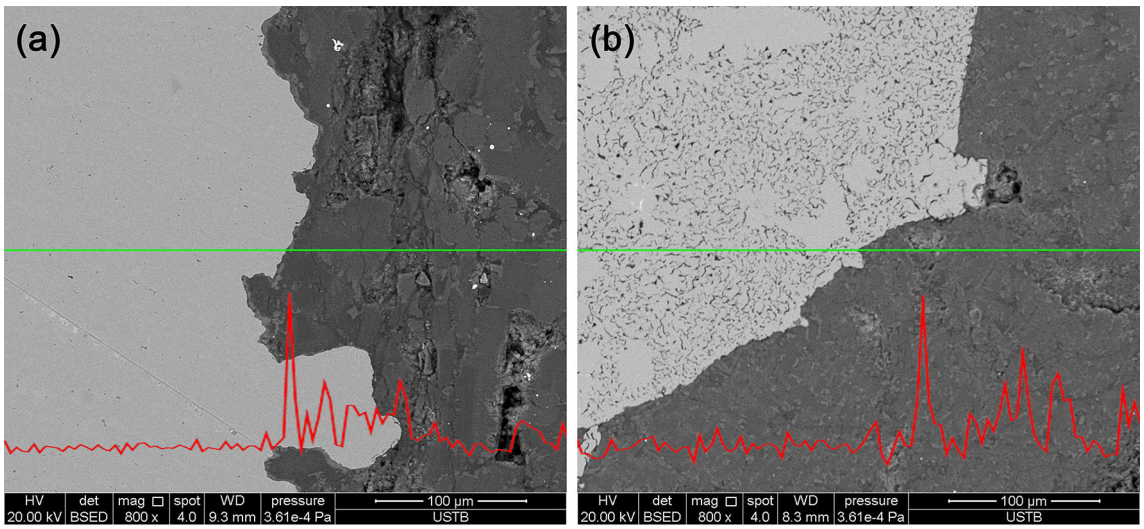

Fig. 7 MLA images of sulfur distribution at slag–metal interface

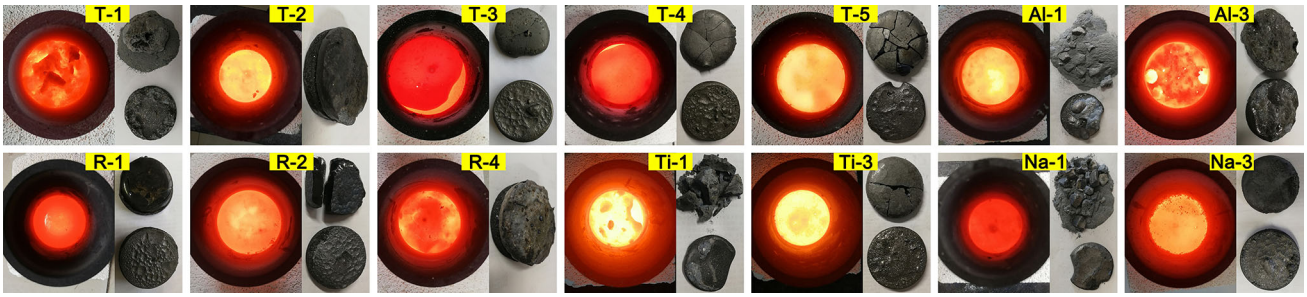

Fig. 8 Melting effect of slag and separation effect of metal from slag

4.6 Melting effect of slag and separation effect of metal from slag

The melting effect of slag and the separation effect of metal from slag are shown in Fig. 8. The melting effect of slag is better as the temperature, Na_2O content, and TiO_2 content increase and basicity decreases. The melting effect of slag is obviously improved when Al_2O_3 content increases from 12.13 to 17.17% (Al-1, T-3), but worsened when Al_2O_3 content increases from 17.17 to 22.27% (T-3, Al-3). This demonstrates that proper Al_2O_3 content promotes the melting of slag, which is consistent with the thermodynamic calculation results. The melting effect of slag and the separation effect of metal from slag are satisfactory when the slag has a basicity of 1.01 and 1.51, and the glass state of slag is obvious (R-1, R-2). The pulverized slag and the poor melting effect are obtained when the low temperature, low Na_2O content and low TiO_2 content are adopted (T-1, T-2, Na-1, Ti-1). Liquid slag is obviously observed with the reactions at 1450 °C and above. At last, the slag–metal interface is complete and smooth, and the separation of metal from slag is satisfactory.

5 Conclusions

1. The thermodynamic calculation results show that Al_2O_3 is beneficial as a flux for lime-based slag. However, the content should be precise. Na_2O promotes the melting effect of slag more effectively than TiO_2.
2. The results of kinetic experiments indicate that the desulfurization rate increases as the temperature, Al_2O_3 content, Na_2O content, and TiO_2 content increase and basicity increases from 1.01 to 1.75, but decreases when basicity increases from 1.75 to 2.02.
3. The melting effect of slag is promoted as the temperature, Na_2O content, and TiO_2 content increase and Al_2O_3 content increases from 12.13 to 17.17%, but worsened as basicity increases and Al_2O_3 content increases from 17.17 to 22.27%. The melting effect of slag is good, and the desulfurization rate is quick within the first 20 min at 1450 °C and above. The slag–metal interface is complete and smooth after the experiment, and the good separation effect of metal from slag is obtained.

4. A kinetic model of hot metal desulfurization has been established, which could calculate the mass transfer coefficient and the mass transfer resistance of sulfur in slag. Total mass transfer coefficients of sulfur were in the range of (5.02–23.78) $\times$ 10^{-7} m s^{-1}. The activation energy was estimated to be 464.06 kJ mol^{-1} at the temperature from 1400 to 1450 °C and 176.35 kJ mol^{-1} at the temperature from 1450 to 1500 °C. The sulfur distribution at the slag–metal interface was observed by using a mineral liberation analyzer. The result shows that the mass transfer of sulfur in slag is the controlling step at high temperature.

Acknowledgements The authors would like to acknowledge the National Key R&D Program of China (No. 2017YFC0210301) and the National Natural Science Foundation of China (No. 51474021) for financial support.

References

[1] J.J. Pak, R.J. Fruehan, Metall. Trans. B 22 (1991) 39–46.
[2] Y.L. Zhang, F.S. Li, R.M. Wang, D.D. Tian, Steel Res. Int. 88 (2017) 1600140.
[3] J.H. Park, D.J. Min, H.S. Song, Metall. Mater. Trans. B 35 (2004) 269–275.
[4] J.F. Xu, L.J. Su, D. Chen, J.Y. Zhang, Y. Chen, J. Iron Steel Res. Int. 22 (2015) 1091–1097.
[5] X.L. Tang, Z.T. Zhang, M. Guo, M. Zhang, X.D. Wang, J. Iron Steel Res. Int. 18 (2011) No. 2, 1–17.
[6] K. Yajima, H. Matsuuran, F. Tsukihashi, ISIJ Int. 50 (2010) 191–194.
[7] H. Park, J.Y. Park, G.H. Kim, I. Sohn, Steel Res. Int. 83 (2012) 150–156.
[8] R.Z. Xu, J.L. Zhang, H.S. Zhang, C.J. Liu, X.Y. Fan, Z.Y. Wang, Iron and Steel 52 (2017) No. 9, 104–109.
[9] I. Sohn, W. Wang, H. Matsuura, F. Tsukihashi, D.J. Min, ISIJ Int. 52 (2012) 158–160.
[10] L.L. Yang, H.M. Wang, X. Zhu, G.R. Li, J. Iron Steel Res. Int. 21 (2014) 745–748.
[11] J.Y. Choi, D.J. Kim, H.G. Lee, ISIJ Int. 41 (2001) 216–224.
[12] Z.F. Tong, J.L. Qiao, X.Y. Jiang, ISIJ Int. 57 (2017) 245–253.
[13] Z.S. Ren, X.J. Hu, K.C. Chou, J. Iron Steel Res. Int. 20 (2013) No. 9, 21–25.
[14] X. Tang, C.S. Xu, ISIJ Int. 35 (1995) 367–371.
[15] J.J. Pak, K. Ito, F.J. Fruehan, ISIJ Int. 29 (1989) 318–323.
[16] X.H. Huang, Iron and steel metallurgical principles, Metallurgical Industry Press, Beijing, 2013.
[17] J.F. Xu, F.X. Huang, X.H. Wang, J. Iron Steel Res. Int. 23 (2016) 784–791.
[18] Q.Y. Han, Kinetics of metallurgical process, Metallurgical Industry Press, Beijing, 1983.
[19] J.K. Jung, J.J. Pak, J. Korean Inst. Met. Mater. 38 (2000) 585–590.
[20] S. Seetharaman, Fundamentals of metallurgy, Woodhead Publishing Limited, Cambridge, 2005.
[21] B. Deo, R. Boom, Fundamentals of steelmaking metallurgy, Prentice Hall, New York, 1993.